DOI:10.1093/jnci/djt168
Advance Access publication August 12, 2013

ARTICLE

Effects of the Selective MPS1 Inhibitor MPS1-IN-3 on Glioblastoma Sensitivity to Antimitotic Drugs

Bakhos A. Tannous, Mariam Kerami, Petra M. Van der Stoop, Nicholas Kwiatkowski, Jinhua Wang, Wenjun Zhou, Almuth F. Kessler, Grant Lewandrowski, Lotte Hiddingh, Nik Sol, Tonny Lagerweij, Laurine Wedekind, Johanna M. Niers, Marco Barazas, R. Jonas A. Nilsson, Dirk Geerts, Philip C. De Witt Hamer, Carsten Hagemann, W. Peter Vandertop, Olaf Van Tellingen, David P. Noske, Nathanael S. Gray, Thomas Würdinger

Manuscript received August 3, 2011; revised November 19, 2012; accepted May 8, 2013.

Correspondence to: Thomas Würdinger, PhD, VU University Medical Center, CCA room 3.34, De Boelelaan 1117, 1081 HV Amsterdam, The Netherlands, (e-mail: t.wurdinger@vumc.nl).

Background Glioblastomas exhibit a high level of chemotherapeutic resistance, including to the antimitotic agents vincristine and taxol. During the mitotic agent-induced arrest, glioblastoma cells are able to perform damage-control and self-repair to continue proliferation. Monopolar spindle 1 (MPS1/TTK) is a checkpoint kinase and a gatekeeper of the mitotic arrest.

Methods We used glioblastoma cells to determine the expression of MPS1 and to determine the effects of MPS1 inhibition on mitotic errors and cell viability in combination with vincristine and taxol. The effect of MPS1 inhibition was assessed in different orthotopic glioblastoma mouse models (n = 3–7 mice/group). MPS1 expression levels were examined in relation to patient survival.

Results Using publicly available gene expression data, we determined that MPS1 overexpression corresponds positively with tumor grade and negatively with patient survival (two-sided *t* test, $P < .001$). Patients with high MPS1 expression (n = 203) had a median and mean survival of 487 and 913 days (95% confidence intervals [CI] = 751 to 1075), respectively, and a 2-year survival rate of 35%, whereas patients with intermediate MPS1 expression (n = 140) had a median and mean survival of 858 and 1183 days (95% CI = 1177 to 1189), respectively, and a 2-year survival rate of 56%. We demonstrate that MPS1 inhibition by RNAi results in sensitization to antimitotic agents. We developed a selective small-molecule inhibitor of MPS1, MPS1-IN-3, which caused mitotic aberrancies in glioblastoma cells and, in combination with vincristine, induced mitotic checkpoint override, increased aneuploidy, and augmented cell death. MPS1-IN-3 sensitizes glioblastoma cells to vincristine in orthotopic mouse models (two-sided log-rank test, $P < .01$), resulting in prolonged survival without toxicity.

Conclusions Our results collectively demonstrate that MPS1, a putative therapeutic target in glioblastoma, can be selectively inhibited by MPS1-IN-3 sensitizing glioblastoma cells to antimitotic drugs.

J Natl Cancer Inst;2013;105:1322–1331

Glioblastoma, the highest grade glioma, is the most common and lethal type of primary brain tumor. Glioblastoma patients have a median survival of less than 15 months following standard of care (1). The main reason for this grim outcome is the rapid tumor growth and invasion of the surrounding brain parenchyma and the failure of standard radiotherapy and temozolomide chemotherapy and additional treatments, such as the use of antimitotic agents, including vincristine and taxol (2,3). Recent advances in expression profiling technologies have allowed the exploratory analysis of differential gene expression in an attempt to identify potential therapeutic targets for cancer therapy. We previously identified a set of kinases to be highly overexpressed in glioma. Apart from WEE1, CDK1, AURKA, and BUBR1, one of the top-rank overexpressed cell cycle-related kinases was MPS1, with an unclear role in glioma (4).

Monopolar spindle 1 (MPS1, also known as TTK), is an evolutionary conserved dual specificity protein kinase that regulates the mitotic spindle checkpoint by monitoring proper chromosome attachment to spindle microtubules (5). As long as unattached kinetochores—the structure where the spindles attach to the chromosomes—are present, the mitotic checkpoint proteins will halt the cell cycle progress until all chromosomes are aligned and stably attached to the spindle. Upon stable orientation of chromosomes in metaphase, chromosome segregation is allowed to proceed (6). MPS1 exerts checkpoint control by redirecting several essential proteins to the kinetochores, including MAD1 and MAD2 (7,8). Furthermore, MPS1 regulates chromosome alignment during metaphase (8–12). Besides its checkpoint function, MPS1 has a probable role in centrosome duplication and

in cytokinesis (5). It is also reported to be involved in the p53-dependent postmitotic checkpoint (13), CHK2 signaling (14), and noncanonical Smad signaling by phosphorylation of Smad2 and Smad3 (15). Misregulation of MPS1 kinase activity results in chromosomal instability and, consequently, in aneuploidy (10). This is a common cause of tumor heterogeneity and poor prognosis in particular for patients with glioma (16–18).

Antimitotic agents such as vincristine and taxol have been in clinical and oncological use for many years and cause mitotic arrest at the metaphase/anaphase boundary. This can result in a decrease in cancer cell proliferation and reduced tumor growth (19–21). However, many cancers, including gliomas, are resistant to these drugs (2,3,22,23). It was previously demonstrated that targeting the mitotic checkpoint through inhibition of MPS1 can lead to accelerated mitosis and apoptosis in cancer cells with no effect on normal fibroblast cells (24). Simultaneous targeting of the mitotic checkpoint and chromosome alignment by inhibition of MPS1 in combination with low doses of the antimitotic drug taxol was shown to result in sensitization of HeLa, HCT-116, LS1740, and U2OS cells to taxol by elevating the frequency of chromosome missegregation (25).

Several MPS1 inhibitors have been developed (24–30). However, compelling data to demonstrate their anticancer activity and safety have not been reported, and so far no MPS1 inhibitor has entered clinical testing in cancer patients. Here we describe the profile of a newly developed, selective, and highly potent MPS1 kinase inhibitor, MPS1-IN-3. We exploit the high expression of MPS1 in glioma and demonstrate that inhibition of this kinase by MPS1-IN-3 sensitizes glioblastoma cells to antimitotic agents in vitro and in vivo, providing a potential therapeutic strategy for the treatment of high-grade gliomas.

Methods

Patient samples

For the REMBRANDT cohort, samples were previously collected from the 14 contributing institutions (National Institutes of Health, Henry Ford Hospital, Thomas Jefferson University, University of California at San Francisco, H. Lee Moffitt Hospital, University of Wisconsin, University of Pittsburgh Medical Center, University of California at Los Angeles, The University of Texas M.D. Anderson Cancer Center, Dana-Farber Cancer Center, Duke University, Johns Hopkins University, Massachusetts General Hospital, and Memorial Sloan Kettering Cancer Center) (33). The samples were provided as snap-frozen sections of areas immediately adjacent to the region used for the histopathologic diagnosis. Initial histopathologic diagnosis was performed at the tissue-collecting institution following World Health Organization (WHO) standards and reviewed by neuropathologists at a central laboratory (33). Additional data on the patient characteristics have been previously pubished (33). In addition, we used the publicly available data of the R2 French glioma cohort (R2.amc.nl) (43). These glioma samples were collected from the tumor archive of the Erasmus University Medical Center, Rotterdam, the Netherlands. All histologic diagnoses were made on formalin-fixed, paraffin-embedded hematoxylin and eosin stained sections and were reviewed blinded to the original diagnosis according to the 2007 WHO classification (43).

Statistical Analysis

The median inhibition concentration (IC_{50}) values were calculated using GraphPad Prism 5.0 (GraphPad Software, La Jolla, CA) using nonlinear curve fitting. Mice survival data were analyzed using the same software, and statistical significance was determined based on log-rank test. Alternatively, the statistical significance level (Student *t* test) was calculated using Microsoft Excel spreadsheets. A *P* value of less than .05 was considered statistically significant. All statistical tests were two-sided.

Additional materials and methods are included in the Supplementary Methods (available online).

Results

Expression Analysis of MPS1 as a Member of an Intricate Network of Mitotic Checkpoint Genes

To determine the expression status of spindle checkpoint genes (6) in glioma, we analyzed the expression of MPS1, BUBR1, AURKA, AURKB, BUB1, PLK1, MAD1, MAD2, and BUB3 using a publicly available dataset containing 152 glioma patients and 23 control subjects (28). Hierarchical clustering analysis was performed to arrange samples and genes into groups based on their expression levels (Figure 1A). Three sample clusters were observed—one represented mainly by normal brain tissue, one by a mixture of glioma subtypes, and one by glioblastoma (Figure 1A). All spindle checkpoint genes analyzed, except for BUB3, were overexpressed in gliomasm, and their expression increased with tumor grade (Figure 1A). These results indicate that MPS1, the most differentially expressed of all mitotic spindle checkpoint genes analyzed, is part of a network of mitotic checkpoint genes that are collectively overexpressed in glioblastoma. To further investigate the correlation between MPS1 gene expression and tumor grade, publicly available gene expression data (28,31,32) were analyzed, and the *P* value for correlation between grade and MPS1 mRNA expression was determined (Figure 1B). MPS1 mRNA expression levels positively corresponded ($P < .001$, as provided by *t* test in the Sun database accessed by Oncomine [http://www.oncomine.com]) to all tumor grades (ie, grade II: $P = 1.22 \times 10^{-6}$; grade III: $P = 2.49 \times 10^{-9}$; grade IV: $P = 1.1 \times 10^{-20}$, as provided by *t* test in the Sun database accessed by Oncomine). We confirmed the overexpression of spindle checkpoint genes in a panel of three non-neoplastic brain (NNB) samples, 15 WHO grade II gliomas, and 15 WHO grade IV gliomas by semiquantitative reverse-transcription polymerase chain reaction (Supplementary Figure 1, A–B, available online), as well as in a panel of glioblastoma cell lines (data not shown). Next, we studied the correlation between MPS1 gene expression levels and patient survival using the publicly available REMBRANDT data (33). As expected on the basis of tumor grade correlation, we found that high MPS1 expression statistically significantly and negatively correlated with survival of glioma patients (log rank $P < .001$) (Figure 1C). Patients with high MPS1 expression (≥3-fold increased MPS1 mRNA expression in glioma as compared with non-neoplastic tissue expression; n = 203) had a median and mean survival of 487 and 913 days (95% CI = 751 to 1075), respectively, and a 2-year survival rate of 35%, whereas patients with intermediate MPS1 expression (<3-fold increased MPS1 mRNA expression in glioma as compared with non-neoplastic tissue expression; n = 140)

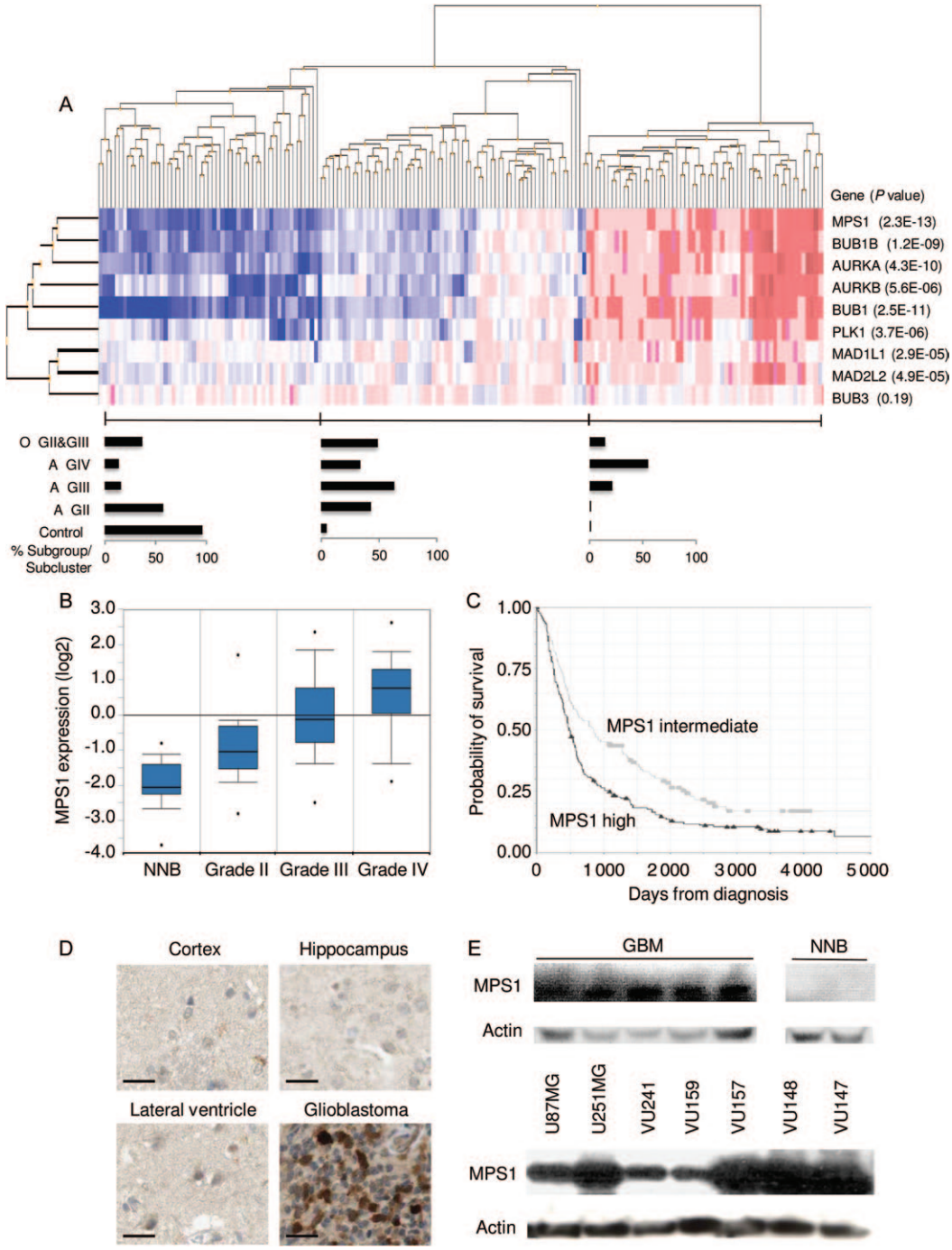

Figure 1. Expression of MPS1 as a member of an intricate network of mitotic checkpoint proteins. **A**) Hierarchical clustering of samples was used to explore the similarities between expression profiles of mitotic spindle checkpoint proteins in glioma. Samples were divided into three clusters. The **bar graphs** indicate the percentage samples within each category: astrocytoma grade II (A GII), grade III (A GIII), and grade IV (A GIV), oligodendroglioma grade II (O GII) and grade III (O GIII), and control. The *P* values indicate the statistical significance of differential expression as calculated using two-sided *t* test. **B**) MPS1 expression positively correlates with glioma grade (Oncomine database). **C**) Overexpression of MPS1 mRNA is associated with decreased survival in adult glioma patients. Kaplan–Meier plots derived from the publicly available REMBRANDT glioma gene expression dataset are grouped according to MPS1 mRNA expression level. **Black curve** represents high MPS1 expression: threefold or greater increase in MPS1 expression compared with non-neoplastic brain samples. **Gray curve** represents intermediate MPS1 expression (less than threefold increase in MPS1 mRNA). Patients with high MPS1 expression (threefold or greater increased MPS1 mRNA expression in glioma as compared with non-neoplastic tissue expression; n=203) had a median and mean survival of 487 and 913 days (95% confidence interval [CI] = 751 to 1075), respectively, and a 2-year survival rate of 35%, whereas the patients with intermediate MPS1 expression (less than threefold increased MPS1 mRNA expression in glioma as compared with non-neoplastic tissue expression; n=140) had a longer median and mean survival of 858 and 1183 days (95% CI = 1177 to 1189), respectively, and a higher 2-year survival rate of 56%. The number of patients at risk at 0, 1000, 2000, 3000, 4000, and 5000 days survival were respectively 203, 52, 23, 14, 7, and 3 for high MPS1 expression and 140, 62, 28, 9, 4, and 1 for intermediate MPS1 expression. **D**) MPS1 protein expression was analyzed by staining of human glioma tissue as well as different regions of normal brain (cortex, ventricle, and hippocampus) as controls, provided by the Human Protein Atlas. **Scale bar** = 50 μm. **E**) Western blot analysis for MPS1 expression using extracts from glioblastoma cell lines, primary cells, and glioblastoma tumor specimens.

had a longer median and mean survival of 858 and 1183 days (95% CI = 1177 to 1189), respectively, and a higher 2-year survival rate of 56% (Figure 1C). These results are explained by the correlation of MPS1 to the different glioma grades (Figure 1A). Similar results were obtained with an independent glioma dataset, which also show the effects of MPS1 expression on the survival within the different glioma subtypes, using the R2 French glioma cohort (R2.amc.nl) (43) (Supplementary Figure 1C, available online). To study MPS1 overexpression at the protein level, we explored the publicly available Human Protein Atlas (http://www.proteinatlas.org). A robust MPS1 protein overexpression was observed in glioblastoma samples as compared with NNB (Figure 1D). To confirm the MPS1 protein expression in glioma samples, we analyzed tissue lysates from NNB and glioblastoma tumor samples by Western blotting. MPS1 protein expression was detected in all glioblastoma samples, whereas no expression could be detected in NNB (Figure 1E). MPS1 protein expression was also confirmed in primary glioblastoma cell cultures and glioblastoma cell lines (Figure 1E).

Effects of Inhibition of MPS1 by RNA Interference on Mitotic Aberrancies and Glioblastoma Cell Proliferation

Previously, it was demonstrated that knockdown of MPS1 causes mitotic abnormalities, confirming its role in normal mitotic progression (34). We thus decided to investigate whether MPS1 knockdown causes abnormal mitosis in glioblastoma cell cultures. We used the H2B-GFP fusion reporter to monitor mitotic aberrancies. U251 glioblastoma cells expressing firefly luciferase (Fluc), and the mCherry fluorescent protein and H2B-GFP (U251-FM-H2B-GFP) were transduced with lentivirus vectors encoding a control shRNA (shCTRL) or a previously validated shRNA (Sigma) directed against MPS1 (shMPS1). Western blot analysis showed efficient MPS1 knockdown in cells expressing shMPS1 as compared with shCTRL (Figure 2A). Fluorescent microscopy showed mitotic errors as indicated by abnormal H2B-GFP localization (Figure 2B). These abnormalities ranged from lobed nuclei and bi- or multinucleated cells caused by defects in cytokinesis to anaphase bridges, chromosome blebs and strings, micronuclei, and lagging chromosomes during anaphase, representing chromosome attachment and segregation defects.

Because MPS1 knockdown resulted in loss of control of the mitotic checkpoint, we determined whether MPS1 knockdown in combination with antimitotic agents could cause a chromosome missegregation phenotype. We therefore treated U251-FM-H2B-GFP cells expressing shCTRL or shMPS1 with the antimitotic agent vincristine or taxol. To investigate the effect of MPS1 knockdown on vincristine-induced cell death, we incubated U251 glioblastoma cells with low doses (3 nM) of vincristine and assessed cell growth after 11 days. Vincristine treatment statistically significantly reduced the number of viable U251-shMPS1 cells as compared with U251-shCTRL cells (t test, $P < .01$) (Figure 2C). Treatment with taxol in combination with MPS1 knockdown demonstrated similar effects as vincristine (Figure 2D). To assess a chromosome missegregation phenotype, U251-FM-H2B-GFP cells expressing shCTRL or shMPS1 and treated with low doses of vincristine (3 nM) or taxol (5 nM) for 7 days were analyzed for nuclear morphology by fluorescence microscopy. As expected, drastic nuclear aberrancies, ranging from lobed nuclei and multinucleated cells suggesting cytokinesis defects to the presence of chromosome bridges and micronuclei, which reflect gross chromosome segregation defects, were observed in shMPS1 cells that had divided in the presence of vincristine or taxol (Figure 2, E and F). To investigate the consequence of MPS1 knockdown on tumor growth in vivo, an orthotopic mouse model was employed. U251-FM cells expressing shCTRL or shMPS1 were used, and tumor growth was monitored by Fluc bioluminescence imaging. MPS1 knockdown resulted in a modest delay of tumor progression (Figure 2G; Supplementary Figure 2A, available online). We then determined whether MPS1 knockdown could sensitize glioblastoma tumors to vincristine-mediated cell death in vivo. U251-FM cells expressing shCTRL or shMPS1 were injected into the brain of mice, and 10 days later, mice were treated with intravenous injections of vincristine (0.5 mg/kg) once per week for 2 weeks. This relatively low dose of vincristine caused a modest reduction of tumor growth. On the other hand, inhibition of MPS1 by shMPS1 caused cessation of tumor growth, demonstrating nearly complete sensitization to vincristine (t test, $P = .003$), as measured by bioluminescence imaging at 3 weeks after implantation of the cells (Figure 2H; Supplementary Figure 2B, available online). Collectively, these data demonstrate that MPS1 knockdown in combination with low doses of antimitotic agents causes lethal chromosome segregation errors, ultimately leading to glioblastoma cell death. These results are consistent with previous findings that connect MPS1-mediated taxol sensitization to chromosome segregation errors (25).

Development of the Selective and Potent MPS1 Inhibitor MPS1-IN-3

Previously, MPS1 inhibitors were identified from an in vitro ATP-site competition-binding assay by screening a diverse library of heterocyclic ATP-site directed kinase scaffolds (26). These inhibitors, MPS1-IN-1 and MPS1-IN-2, represented distinct chemical scaffolds; however, both displayed potent activity against MPS1. In the course of our medicinal chemistry efforts, we discovered a closely related analog of MPS1-IN-1, MPS1-IN-3, which potently inhibited MPS1 kinase activity with an IC_{50} of 50 nM (Supplementary Table 1, available online). To arrive at MPS1-IN-3, the pyrollopyridine core of MPS1-IN-1 was replaced with a purine core scaffold (Figure 3A; Supplementary Methods, available online). This chemical modification resulted in nearly a fivefold increase in activity against MPS1 in a biochemical assay (Supplementary Figure 3, available online). To test whether MPS1-IN-3 abrogates the spindle checkpoint, we challenged U2OS cells arrested in mitosis with increasing concentration of MPS1-IN-3. Silencing of the spindle checkpoint, a surrogate readout of MPS1 activity, was assessed by monitoring the stability of cyclin B (Figure 3B). The levels of cyclin B, a marker of mitotic cells, dropped with increasing concentration of MPS1-IN-3 but was reversed by addition of the proteasome inhibitor MG132 (Figure 3B). Complete checkpoint abrogation was observed with 2 μM of MPS1-IN-3. Downregulation of this mitotic marker indicated that MPS1-IN-3 caused a dose-dependent escape from a checkpoint-mediated mitotic arrest. In addition, we confirmed functional MPS1 kinase inhibition in U251 glioblastoma cells by analyzing the phosphorylation levels of the MPS1 target Smad2 by Western blotting using MPS1-IN-3 at

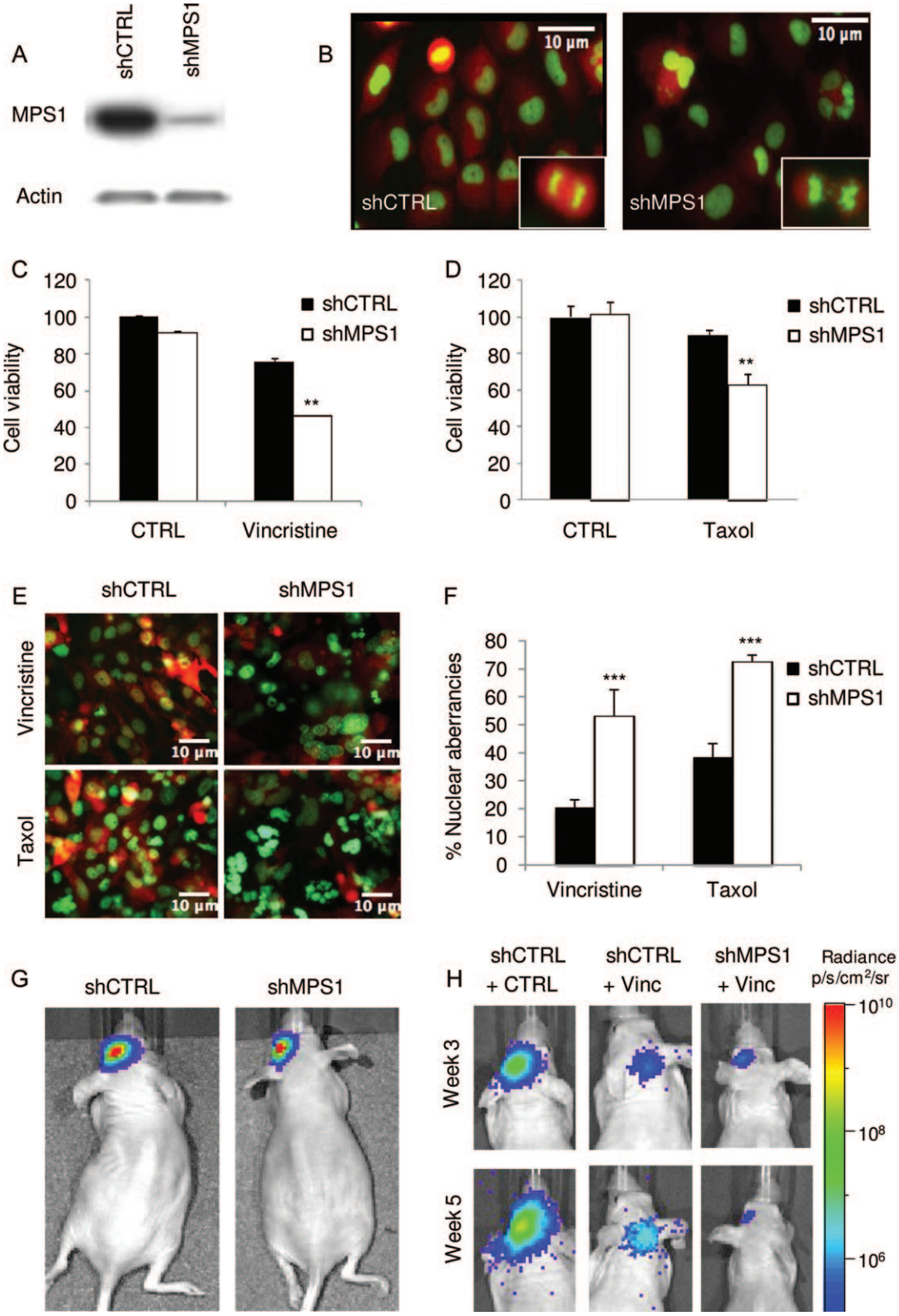

Figure 2. The effect of inhibition of MPS1 by RNA interference on mitotic aberrancies and glioblastoma cell proliferation. **A**) Western blot analysis showing MPS1 knockdown in U251 cells using shMPS1. **B**) U251-shCTRL and U251-shMPS1 cells expressing H2B-GFP were analyzed for changes in nuclear morphology using fluorescence microscopy. **Scale bar** = 10 µm. **C** and **D**) U251 cells expressing shMPS1 or shCTRL were treated with low concentrations of vincristine (3 nM) or taxol (5 nM), and 11 days after addition, cell viability was assessed using the crystal violet assay. Data shown as average ± standard deviation. ***P* < .01, two-sided *t* test. **E**) U251-FM-H2B-GFP cells expressing shCTRL or shMPS1 were treated with 3 nM of vincristine or 5 nM of taxol for 7 days, after which cells were analyzed using fluorescence microscopy for nuclear morphology. **Scale bar** = 10 µm. **F**) Quantitation of nuclear aberrancies visualized in (**E**). Data shown as average ± standard deviation. ****P* < .001, two-sided *t* test. **G**) Nude mice (n = 3) were injected intracranially with U251-FM-shCTRL or -shMPS1 cells. Tumor growth was analyzed by firefly luciferase bioluminescence imaging at week 7. **H**) Similar group of mice (n = 3) as in (**G**) treated with 0.5 mg/kg of vincristine (Vinc) or DMSO (CTRL).

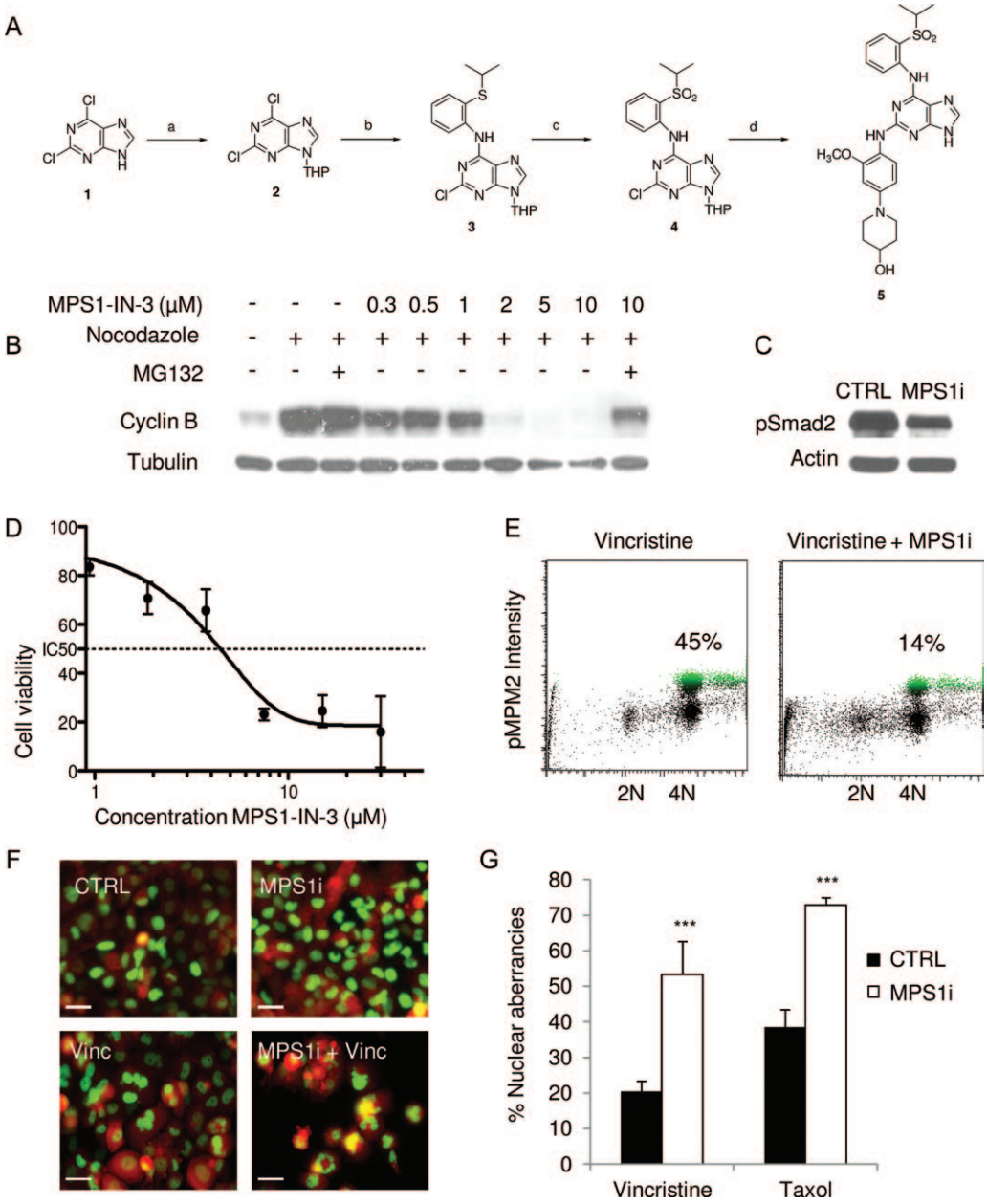

Figure 3. Development of the selective and potent MPS1 inhibitor MPS1-IN-3. **A**) Chemical development of MPS1-IN-3. Compound 1—2,6-dichloro-9*H*-purine—was first converted by reaction a to compound 2—2,6-dichloro-9-(tetrahydro-2H-pyran-2-yl)-9H-purine—then by reaction b to compound 3—2-chloro-N-(2-(isopropylthio)phenyl)-9-(tetrahydro-2*H*-pyran-2-yl)-9*H*-purin-6-amine—and reaction c to product 4—2-chloro-N-(2-(isopropylsulfonyl)phenyl)-9-(tetrahydro-2H-pyran-2-yl)-9H-purin-6-amine—to finally reach desired product 5 by reaction d—1-(4-(6-(2-(isopropylsulfonyl)phenylamino)-9H-purin-2-ylamino)-3-ethoxyphenyl)piperidin-4-ol (MPS1-IN-3). Reactions, reagents, and conditions are described in the Supplementary Experimental Procedures (available online). **B**) Western blot analysis of cyclin B in U2OS cells treated with nocodazole, MPS1-IN-3, and/or MG132. **C**) Western blot analysis of Smad2 phosphorylation in U251 cells incubated with 5 μM of MPS1-IN-3 (MPS1i) and vincristine. **D**) Dose–response curve of MPS1-IN-3 on U251 glioblastoma cells as analyzed by cell counts. Data shown as average ± standard deviation. **E**) Fluorescence activated cell sorting analysis of pMPM2 in U251 cells 24 hour after addition of 5 μM of MPS1-IN-3 (MPS1i) and vincristine. Percentages indicate cells in mitotic arrest. **F**) U251-FM-H2B-GFP cells were treated with DMSO (CTRL) or MPS1-IN-3 (MPS1i) in combination with vincristine or taxol. The nuclear morphology was assessed with fluorescence microscopy and quantitated in (**G**). **Scale bar** = 10 μm. The experiment was performed in triplicate. Shown are mean averages, and **error bars** indicate standard deviation.

5 μM (Figure 3C), and MPS1-IN-3 inhibited the proliferation of U251 glioblastoma cells as determined by cell counting with an IC_{50} value of approximately 5 μM (Figure 3D), demonstrating improved effects over the inhibitors MPS-IN-2 and AZ-3146 (Supplementary Figure 3, available online). In addition, U251 cells were subjected to pMPM2 fluorescence activated cell sorting analysis in the presence of vincristine, demonstrating a reduction in the number of U251 cells in vincristine-induced mitotic arrest after MPS1-IN-3 treatment (Figure 3E). To determine whether MPS1 inhibition by MPS1-IN-3 in combination with antimitotic agents causes chromosome missegregation phenotypes, we treated U251-FM-H2B-GFP cells with MPS1-IN-3 at 5 μM and low doses of

vincristine (3 nM) or taxol (5 nM), and after 1 week, cells were analyzed for nuclear morphology by fluorescence microscopy. Similar to MPS1 knockdown, drastic nuclear aberrancies, including lobed nuclei and multinucleated cells, and micronuclei reflecting gross chromosome segregation defects were observed in U251 cells treated with MPS1-IN-3 in the presence of vincristine or taxol (Figure 3, F and G). In conclusion, MPS1-IN-3 is a selective and potent MPS1 inhibitor with phenotypic consequences similar to those reported for published MPS1 inhibitors such as MPS1-IN-1, MPS1-IN-2, and AZD3146 (26,29,30).

Effects of Inhibition of MPS1 by MPS1-IN-3 on Sensitivity of Glioblastoma Cells to Vincristine In Vitro and In Vivo

Next, we determined the effect of MPS1-IN-3 on U251 and U87 glioblastoma cell lines and VU147 primary glioblastoma cells as well as GBM8 primary neurospheres in the presence or absence of vincristine. Treatment with MPS1-IN-3 at 5 μM sensitized all glioblastoma cells to 3 nM of vincristine as measured by cell counts 11 days posttreatment (Figure 4A). To investigate the consequence of MPS1-IN-3 in combination with vincristine on tumor growth in vivo, an orthotopic glioblastoma mouse model was employed using U251-FM cells. U251-FM cells were stereotactically injected into the brain of nude mice. Ten days postinjection, 2 mg/kg of MPS1-IN-3 and/or 0.5 mg/kg of vincristine were administered concomitantly by intravenous injections twice per week for 3 weeks. Tumor growth was monitored by Fluc imaging, and mice were monitored for survival and for any signs of treatment toxicity. A statistically significant decrease in Fluc bioluminescence signal and therefore tumor volume and an increase in survival were observed in mice treated with MPS1-IN-3 in combination with vincristine as compared with no treatment, in contrast with mice treated with MPS1-IN-3 or vincristine alone (t test, $P < .05$) (Figure 4, B–D). To validate these results in a more clinically relevant model, we employed the orthotopic primary GBM8-FM neurosphere model, which infiltrates the mouse brain in a process similar to that in human GBM patients (35) using the same treatment conditions. A statistically significant decrease in bioluminescence signal and increased survival were observed in mice treated with MPS1-IN-3 in combination with vincristine, in contrast with mice treated with vincristine or MPS1-IN-3 alone or with the no treatment controls (t test, $P < .05$) (Figure 4, E–G). An initial increase in Fluc signal was observed in the first week of vincristine monotreatment in the U251 model. However, we did not observe this phenomenon in the GBM8 model. The differences in growth inhibition of the U251 and GBM8 models we attribute to the different nature of the U251 GBM cell line and the primary GBM8 stemlike cells. We noticed no toxicity upon treatment of the mice, as was confirmed by additional toxicity analysis. C57BL/6-naive mice were injected with either vehicle, vincristine, MPS1-IN-3, or a combination of vincristine and MPS1-N3 (similar doses to what we used for tumor treatment in vivo) on day 1 and day 3. On day 4, blood was collected and analyzed for complete blood count, a comprehensive chemistry panel, and a liver enzyme panel, revealing no signs of toxicity (data not shown). Altogether these results demonstrate that MPS1-IN-3 sensitizes glioblastoma cells to vincristine both in vitro and in murine tumor models.

Discussion

Most high-grade gliomas are resistant to conventional and experimental therapies including antimitotic agents such as taxol and vincristine (2,3). The MPS1 kinase controlled mitotic checkpoint is an essential factor in determining the response of tumor cells to antimitotic drugs (36–39). Here, we demonstrate that MPS1 is a highly expressed mitotic checkpoint protein in glioma and a potential therapeutic target in high-grade gliomas. We designed a new selective MPS1 inhibitor that effectively sensitizes glioblastomas to vincristine in two orthotopic glioblastoma xenograft models.

Limitations of this study include the fact that MPS1-IN-3 was tested in a limited number of glioblastoma cell lines in combinations with vincristine. It would be of interest to further characterize the effect of MPS1 inhibition on a vast number of primary glioblastoma cell lines and to determine whether certain cellular expression patterns correspond to the effectiveness of the drug. The same accounts for the in vivo studies, in which the U251 glioblastoma cell line and the GBM8 primary glioblastoma stemlike cell models were used. In addition, although effects of statistical significance were measured in vivo, the exact pharmacodynamics and kinetics of MPS1-IN-3 remain to be investigated. This includes studying the half-life of the drug, crossing of the blood brain barrier, drug pump substrate specificity, and functional target engagement (eg, by pSmad2 analysis) in different dosing schemes in combination with vincristine. Tumor heterogeneity may play a role in the treatment response to MPS1-IN-3, and it would be of interest to study the effects of MPS1-IN-3 on different samples of the same tumor. So far, it is unclear whether resistance to MPS1 inhibition can occur in glioblastoma cells. Studies performing long-term exposure of glioblastoma cells to MPS1-IN-3 and vincristine could reveal whether such mechanisms occur and, possibly, how this could be overcome. Finally, we observed minimal toxicity in our in vivo studies. However, we only studied toxicity in two different glioblastoma in vivo models. Additional dose-escalating toxicity studies are warranted to optimize the combination of MPS1-IN-3 in combination with vincristine.

Vincristine has been used in different combination regiments (procarbazine, lomustine, and vincristine) for the therapy of high-grade oligodendroglioma and anaplastic oligodendroglioma (40,41). Indeed, a recent meta-analysis emphasized the role of vincristine in high-grade glioma therapy by showing that patient cohorts treated with vincristine-containing regimens had statistically significant survival advantage over cohorts treated with other chemotherapy drugs (42). However, the efficacy of vincristine in glioma treatment has been hampered by toxicity such as polyneuropathy and hematological side effects. Combination of vincristine with MPS1 inhibitors may not only potentiate the antitumor effect of vincristine but may also ameliorate the notorious side effects by allowing reduced vincristine dosing, although treatment of both normal and cancer cells with MPS1 inhibitors causes severe chromosome segregation defects and aneuploidy, suggesting that the tolerability of chronic administration of such agents warrants further investigation. In conclusion, our results demonstrate that MPS1 may be a promising therapeutic target for high-grade glioma therapy and that MPS1 inhibition by MPS1-IN-3 efficiently sensitizes glioblastoma cells to antimitotic agents.

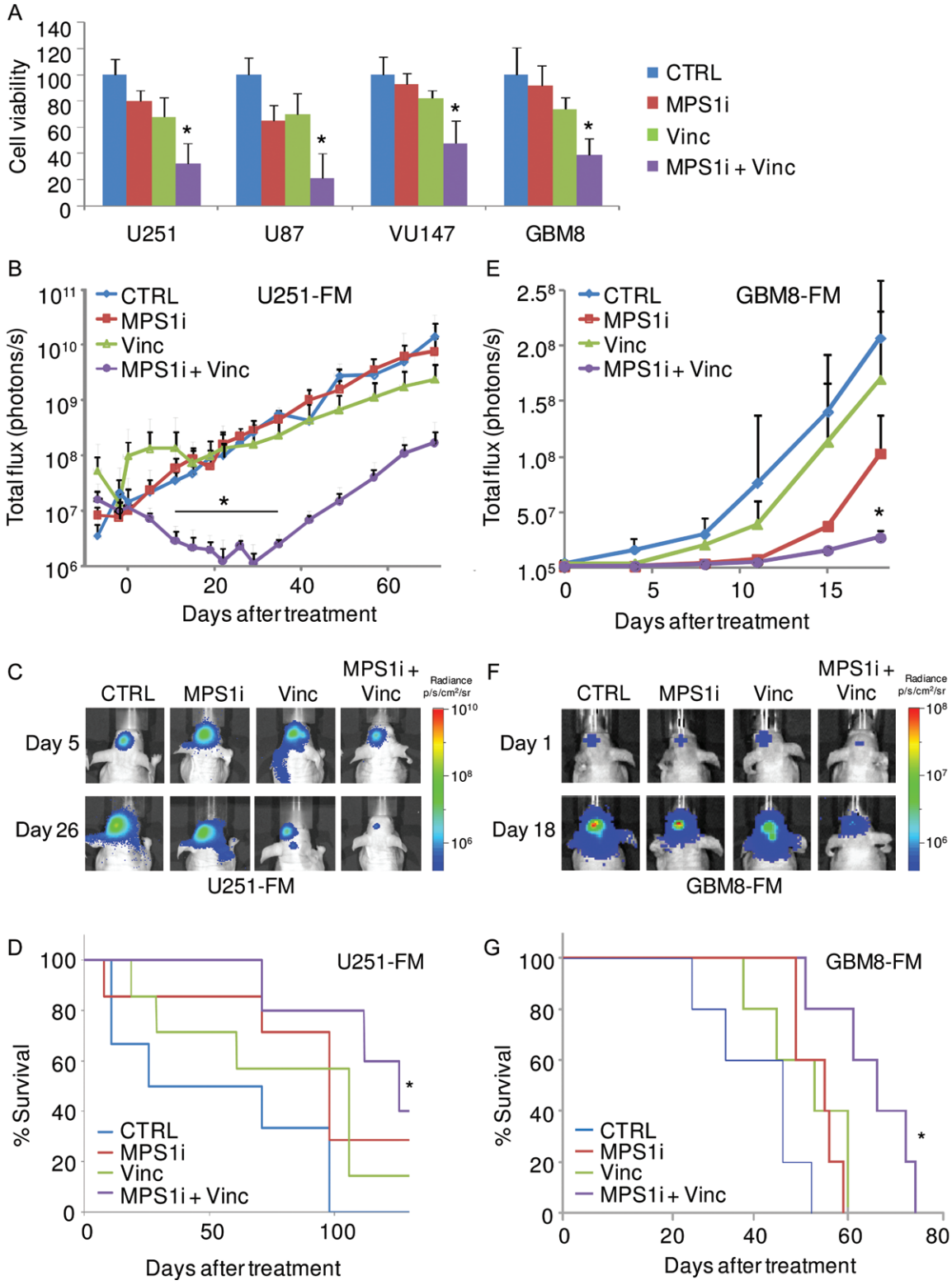

Figure 4. Effect of inhibition of MPS1 by MPS1-IN-3 on sensitivity of glioblastoma cells to vincristine in vitro and in vivo. **A**) Cell viability analysis of glioblastoma cells 11 days after treatment with MPS1-IN-3 with and without vincristine. Data shown as average ± standard deviation. *$P <$ .05, two-sided *t* test. **B** and **C**) Intracranial U251-FM tumor growth monitored by firefly luciferase (Fluc) bioluminescence imaging, n = 5–7. Mice were injected intravenously with vehicle (CTRL), 0.5 mg/kg of vincristine (Vinc), 2 mg/kg of MPS1-IN-3 (MPS1i), or both vincristine and MPS1-IN-3, twice a week for 3 weeks. Data shown as mean Fluc flux ± standard error of the mean. *$P <$ .05, two-sided *t* test. **D**) Survival analysis of (**B**) and (**C**). Number of mice at risk at 0, 50, 100, and 125 days after injection of U251-FM cells were respectively 6, 4, 2, and 2 (CTRL); 7, 6, 5, and 1 (Vinc) 7, 7, 5, and 2 (MPS1i); and 5, 5, 5, and 3 (Vinc+MPS1i). *$P <$ .01, two-sided log-rank test. **E** and **F**) Intracranial GBM8-FM tumor growth monitored by Fluc bioluminescence imaging and treated as in (**B–D**), n = 5. Data shown as mean ± standard error of the mean. *$P <$ .05, two-sided *t* test. **G**) Survival analysis of (**E**) and (**F**). Number of mice at risk at day 0, 20, 40, 60, and 80 days after injection of GBM8-FM cells were respectively 5, 4, 1, 0, and 0 (CTRL); 5, 5, 3, 0, and 0 (Vinc) 5, 5, 5, 0, and 0 (MPS1i); and 5, 5, 5, 4, and 0 (Vinc+MPS1i). *$P <$ .01, two-sided log-rank test.

References

1. Stupp R, Mason WP, van den Bent MJ, et al. Radiotherapy plus concomitant and adjuvant temozolomide for glioblastoma. *N Engl J Med*. 2005;352(10):987–996.
2. Thomas D, Brada M, Stenning S. Randomized trial of porcarbazine, lomustine, and vincristine in the adjuvant treatment of high-grade astrocytoma: A medical research council trial. *J Clin Oncol*. 2001;19(2):509–518.
3. Fetell MR, Grossman SA, Fisher JD, et al. Preirradiation paclitaxel in glioblastoma multiforme: efficacy, pharmacology, and drug interactions. New Approaches to Brain Tumor Therapy Central Nervous System Consortium. *J Clin Oncol*. 1997;15(9):3121–3128.
4. Mir SE, de Witt Hamer PC, Krawczyk PM, et al. In silico analysis of kinase expression identifies WEE1 as a gatekeeper against mitotic catastrophe in glioblastoma. *Cancer Cell*. 2010;18(3):244–257.
5. Fisk HA, Mattison CP, Winey M. A field guide to the Mps1 family of protein kinases. *Cell Cycle*. 2004;3(4):439–442.
6. Musacchio A and Salmon ED. The spindle-assembly checkpoint in space and time. *Nat Rev Mol Cell Biol*. 2007;8(5):379–393.
7. Tighe A, Staples O, Taylor S. Mps1 kinase activity restrains anaphase during an unperturbed mitosis and targets Mad2 to kinetochores. *J Cell Biol*. 2008;181(6):893–901.
8. Maciejowski J, George KA, Terret ME, et al. Mps1 directs the assembly of Cdc20 inhibitory complexes during interphase and mitosis to control M phase timing and spindle checkpoint signaling. *J Cell Biol*. 2010;190(1):89–100.
9. Maure JF, Kitamura E, Tanaka TU. Mps1 kinase promotes sister-kinetochore bi-orientation by a tension-dependent mechanism. *Curr Biol*. 2007;17(24):2175–2182.
10. Jelluma N, Brenkman AB, McLeod I, et al. Chromosomal instability by inefficient Mps1 auto-activation due to a weakened mitotic checkpoint and lagging chromosomes. *PLoS One*. 2008;3(6):e2415.
11. Jelluma N, Brenkman AB, van den Broek NJ, et al. Mps1 phosphorylates borealin to control aurora B activity and chromosome alignment. *Cell*. 2008;132(2):233–246.
12. Santaguida S, Tighe A, D'Alise AM, Taylor SS, Musacchio A. Dissecting the role of MPS1 in chromosome biorientation and the spindle checkpoint through the small molecule inhibitor reversine. *J Cell Biol*. 2010;190(1):73–87.
13. Huang YF, Chang MD, Shieh SY. TTK/hMps1 mediates the p53-dependent postmitotic checkpoint by phosphorylating p53 at Thr18. *Mol Cell Biol*. 2009;29(11):2935–2944.
14. Yeh YH, Huang YF, Lin TY, Shieh SY. The cell cycle checkpoint kinase CHK2 mediates DNA damage-induced stabilization of TTK/hMps1. *Oncogene*. 2009;28(10):1366–1378.
15. Zhu S, Wang W, Clarke DC, Liu X. Activation of Mps1 promotes transforming growth factor-beta-independent Smad signaling. *J Biol Chem*. 2007;282(25):18327–18338.
16. Nishizaki T, Harada K, Kubota H, et al. Chromosome instability in malignant astrocytic tumors detected by fluorescence in situ hybridization. *J Neurooncol*. 2002;56(2):159–165.
17. Zeng WF, Navaratne K, Prayson RA, Weil RJ. Aurora B expression correlates with aggressive behaviour in glioblastoma multiforme. *J Clin Pathol*. 2007;60(2):218–221.
18. Lengauer C, Kinzler KW and Vogelstein B. Genetic instabilities in human cancers. *Nature*. 1998;396(6712):643–649.
19. Jordan MA, Thrower D, Wilson L. Mechanism of inhibition of cell proliferation by Vinca alkaloids. *Cancer Res*. 1991;51(8):2212–2222.
20. Jordan MA, Thrower D, Wilson L. Effects of vinblastine, podophyllotoxin and nocodazole on mitotic spindles. Implications for the role of microtubule dynamics in mitosis. *J Cell Sci*. 1992;102(Pt 3):401–416.
21. Jordan MA, Toso RJ, Thrower D, Wilson L. Mechanism of mitotic block and inhibition of cell proliferation by taxol at low concentrations. *Proc Natl Acad Sci U S* A. 1993;90(20):9552–9556.
22. Yusuf RZ, Duan Z, Lamendola DE, Penson RT, Seiden MV. Paclitaxel resistance: molecular mechanisms and pharmacologic manipulation. *Curr Cancer Drug Targets*. 2003;3(1):1–19.
23. Goncalves A, Braguer D, Kamath K, et al. Resistance to taxol in lung cancer cells associated with increased microtubule dynamics. *Proc Natl Acad Sci U S* A. 2001;98(20):11737–11742.
24. Colombo R, Caldarelli M, Mennecozzi M, et al. Targeting the mitotic checkpoint for cancer therapy with NMS-P715, an inhibitor of MPS1 kinase. *Cancer Res*. 2010;70(24):10255–10264.
25. Janssen A, Kops GJ, Medema RH. Elevating the frequency of chromosome mis-segregation as a strategy to kill tumor cells. *Proc Natl Acad Sci U S* A. 2009;106(45):19108–19113.
26. Kwiatkowski N, Jelluma N, Filippakopoulos P, et al. Small-molecule kinase inhibitors provide insight into Mps1 cell cycle function. *Nat Chem Biol*. 2010;6(5):359–368.
27. Dorer RK, Zhong S, Tallarico JA, et al. A small-molecule inhibitor of Mps1 blocks the spindle-checkpoint response to a lack of tension on mitotic chromosomes. *Curr Biol*. 2005;15(11):1070–1076.
28. Sun L, Hui AM, Su Q, et al. Neuronal and glioma-derived stem cell factor induces angiogenesis within the brain. *Cancer Cell*. 2006;9(4):287–300.
29. Hewitt L, Tighe A, Santaguida S, et al. Sustained Mps1 activity is required in mitosis to recruit O-Mad2 to the Mad1-C-Mad2 core complex. *J Cell Biol*. 2010;190(1):25–34.
30. Lan W, Cleveland DW. A chemical tool box defines mitotic and interphase roles for Mps1 kinase. *J Cell Biol*. 2010;190(1):21–24.
31. Freije WA, Castro-Vargas FE, Fang Z, et al. Gene expression profiling of gliomas strongly predicts survival. *Cancer Res*. 2004;64(18):6503–6510.
32. Bredel M, Bredel C, Juric D, et al. Functional network analysis reveals extended gliomagenesis pathway maps and three novel MYC-interacting genes in human gliomas. *Cancer Res*. 2005;65(19):8679–8689.
33. National Cancer Institute. 2005. REMBRANDT Home Page. http://rembrandt.nci.nih.gov. Accessed May 2, 2013.
34. Fisk HA, Mattison CP, Winey M. Human Mps1 protein kinase is required for centrosome duplication and normal mitotic progression. *Proc Natl Acad Sci U S* A. 2003;100(25):14875–14880.
35. Wakimoto H, Kesari S, Farrell CJ, et al. Human glioblastoma-derived cancer stem cells: establishment of invasive glioma models and treatment with oncolytic herpes simplex virus vectors. *Cancer Res*. 2009;69(8):3472–3481.
36. Kops GJ, Foltz DR, Cleveland DW. Lethality to human cancer cells through massive chromosome loss by inhibition of the mitotic checkpoint. *Proc Natl Acad Sci U S* A. 2004;101(23):8699–8704.
37. Michel L, Diaz-Rodriguez E, Narayan G, et al. Complete loss of the tumor suppressor MAD2 causes premature cyclin B degradation and mitotic failure in human somatic cells. *Proc Natl Acad Sci U S* A. 2004;101(13):4459–4464.
38. Kim M, Liao J, Dowling ML, et al. TRAIL inactivates the mitotic checkpoint and potentiates death induced by microtubule-targeting agents in human cancer cells. *Cancer Res*. 2008;68(9):3440–3449.
39. Lee EA, Keutmann MK, Dowling ML, et al. Inactivation of the mitotic checkpoint as a determinant of the efficacy of microtubule-targeted drugs in killing human cancer cells. *Mol Cancer Ther*. 2004;3(6):661–669.
40. Soffietti R, Ruda R, Bradac GB, Schiffer D. PCV chemotherapy for recurrent oligodendrogliomas and oligoastrocytomas. *Neurosurgery*. 1998;43(5):1066–1073.
41. Nieder C, Mehta MP, Jalali R. Combined radio- and chemotherapy of brain tumours in adult patients. *Clin Oncol (R Coll Radiol)*. 2009;21(7):515–524.
42. Aydin B, Patil M, Bekele N, Wolff JE. Vincristine in high-grade glioma. *Anticancer Res*. 2010;30(6):2303–2310.
43. Gravendeel LA, Kouwenhoven MC, Gevaert O, et al. Intrinsic gene expression profiles of gliomas are a better predictor of survival than histology. *Cancer Res*. 2009;69(23):9065–72.

Funding

This work was supported partly by the National Institues of Health/National Institute of Neurological Disorders and Stroke (1R01NS064983 to BAT); STOPhersentumoren.nl (to PMVdS); NWO-VIDI (to TW); and the National Institutes of Health (U54 HG006097-02 to NSG).

Notes

In memoriam of Mariam Kerami. B.A. Tannous, M. Kerami, and P.M. van der Stoop contributed equally to this work.

The study sponsor had no role in the design of the study; the collection, analysis, and interpretation of the data; the writing of the manuscript; and the decision to submit the manuscript for publication.

We are grateful to Stefanie Gerngras and Siglinde Kühnel for technical assistance. We would also like to thank Jian Teng and Sayedali Hejazi for their help with toxicity analysis.

Affiliations of authors: Neuroscience Center and Molecular Neurogenetics Unit, Departments of Neurology, Harvard Medical School, Boston, MA (BAT, MK, GL, MB, TW); Center for Molecular Imaging Research, Department of Radiology, Massachusetts General Hospital, Boston, MA (BAT, MK, GL, MB, TW); Neuroscience Program, Harvard Medical School, Boston, MA(BAT, MK, GL, MB, TW); Neuro-oncology Research Group, Department of Neurosurgery, VU University Medical Center, Amsterdam, The Netherlands (MK, PMVdS, LH, NS, LW, JMN, MB, RJAN, PCDWH, WPV, DPN, TW); Department of Cancer Biology, Dana Farber Cancer Institute, Boston, MA (NK, JW, WZ, NSG); and Department of Biological Chemistry and Molecular Pharmacology, Harvard Medical School, Boston, MA (NK, JW, WZ, NSG); Department of Neurosurgery, Tumorbiology Laboratory, University of Würzburg, Würzburg, Germany (AFK, CH); Department of Radiation Sciences, Oncology, Umeå University, Umeå, Sweden (RJAN); Department of Pediatric Oncology/Hematology, Sophia Children's Hospital, Erasmus University Medical Center, Rotterdam, The Netherlands (DG); Department of Clinical Chemistry/Preclinical Pharmacology, The Netherlands Cancer Institute, Antoni van Leeuwenhoek Hospital, Amsterdam, The Netherlands (OVT).